DRUG DEVELOPMENT RESEARCH 67:61–69 (2006)

DDR

Research Article

Discrete Thermally Responsive Hydrogel-Coated Gold Nanoparticles for Use as Drug-Delivery Vehicles

Jun-Hyun Kim and T. Randall Lee*

Department of Chemistry, University of Houston, 4800 Calhoun Road, Houston, Texas

Strategy, Management and Health Policy				
Enabling Technology, Genomics, Proteomics	Preclinical Research	Preclinical Development Toxicology, Formulation Drug Delivery, Pharmacokinetics	Clinical Development Phases I-III Regulatory, Quality, Manufacturing	Postmarketing Phase IV

ABSTRACT This report describes the development of optically responsive gold nanoparticles (~60 nm in diameter) coated with a thermally responsive biocompatible hydrogel overlayer (20–90 nm thick). The hydrogel consists of a mixture of N-isoproprylacrylamide and acrylic acid; this copolymer can be tailored to exhibit a lower critical solution temperature (LCST) slightly above physiological temperature. When the temperature is raised above the LCST, the hydrogel polymer shrinks dramatically; in contrast, when the temperature is lowered below the LCST, the hydrogel expands to a fully swollen structure. These hybrid nanoparticles were designed for the purpose of developing an optically modulated drug-delivery system that responds to ambient changes in temperature. Specifically, drug-impregnated hydrogel coatings can be photothermally activated by exposure to light that can be absorbed by the plasmon resonance of the gold nanoparticle cores. The studies described here demonstrate that these new hybrid core-shell nanoparticles can be reproducibly prepared by surfactant-free emulsion polymerization (SFEP) and that their structural responses to external stimuli are consistent with our objective of photothermal drug delivery. Drug Dev. Res. 67:61–69, 2006. © 2006 Wiley-Liss, Inc.

Key words: gold; nanoparticle; biocompatible; hydrogel; photothermal; drug delivery

INTRODUCTION

Many recent studies have focused on nanometer-sized particles for the purpose of developing new optical and electrical devices [Alivisatos, 1996; Maier et al., 2001]. Studies of inorganic nanostructured materials have received great attention due to their unique electrical and optical properties as well as their biocompatible nature [Kreibig and Vollmer, 1995]. However, significant new progress in the modification of nanoparticles is necessary for the further development of nanoscale components and functional materials. Metal nanoparticles including platinum, silver, copper, and especially gold are particularly well suited for these nanoparticle-based optical and biological applications because of their ability to absorb and/or scatter light [Bohren et al., 1998; Teranishi and Miyake, 1998; Quanroni et al., 1999; Chen et al., 2001; Clark et al., 2000].

Metallic gold is known as a biocompatible material and is used in many applications, ranging from dental surgery to treatments for arthritis [Merchant, 1998]. Gold nanoparticles are attractive for use as components in optically-responsive biomaterials due to their biocompatible nature and their unique optical properties in the visible range of the electromagnetic spectrum [Sun and Xia, 2002]. A

Grant sponsor: National Science Foundation; Grant number: ECS-0404308; Grant sponsor: National Aeronautics and Space Administration; Grant number: NCC-1-02038; Grant sponsor: Robert A. Welch Foundation; Grant number: E-1320.

*Correspondence to: T. Randall Lee, Department of Chemistry, University of Houston, 4800 Calhoun Road, Houston, TX 77204-5003. E-mail: trlee@uh.edu

Published online in Wiley InterScience (www.interscience.wiley.com). DOI: 10.1002/ddr.20068

specific objective of our research is to prepare discrete biocompatible hydrogel-coated gold nanoparticles that undergo structural changes in aqueous solution upon exposure to light.

Hydrogels are important in various technological applications, such as chemical separations, drug delivery, and catalysis [Pelton, 2000; Jeong et al., 1997; Bergbreiter et al., 1998]. Hydrogels are crosslinked polymer frameworks that are easily dispersed in aqueous solution. They undergo reversible volume transitions that are mainly dependent on the lower critical solution temperature (LCST) as well as other chemical or physical stimuli [Schild et al., 1990; Saunders and Vincent, 1996; Zhou and Chu, 1998]. Numerous thermo- and pH-responsive hydrogel particles have been developed [Jones and Lyon, 2000]. In particular, hydrogel-based composite particles are used in applications ranging from enhanced oil recovery, to controlled reversible flocculation, and to the uptake and release of heavy metals [Snowden et al., 1993].

A specific type of hydrogel material based on poly (N-isopropylacrylamide) (NIPAM) has been widely studied because of its remarkable thermosensitivity [Pelton, 2000; Jones and Lyon, 2003a,b; Zhu et al., 2004; Pelton et al., 1989]. However, homo-polymer NIPAM hydrogels have limited applications because thermally-induced volume changes of these materials occur at a fixed LCST of ~32°C [Snowden et al., 1996]. This limitation can be circumvented by incorporating acrylic acid (AAc) or acrylamide (AAm) moieties into the polymer backbone, which can shift the LCST of the copolymer hydrogels anywhere from 32 to 60°C depending on the ratio of components [Snowden et al., 1996]. The presence of AAc or AAm in the poly-NIPAM hydrogels both increases the LCST and causes the hydrogel particles to undergo a discontinuous transition and a large change in volume [Yoshida et al., 1994]. These materials are partially desolvated above the LCST, but become highly water-swollen, depending on the polymer structure, when cooled below the LCST. Furthermore, NIPAM-based hydrogels exhibit a continuously reversible swelling-deswelling transition as a function of both temperature and pH.

To effect photothermally-modulated volume transitions in hydrogel polymers, photosensitive moieties such as dyes or metal nanoparticles have been incorporated into the hydrogel matrix [Zhu et al., 2004; Nayak and Lyon, 2004; Jones and Lyon, 2003a,b]. In the work described here, we grow a hydrogel layer around a gold nanoparticle core and demonstrate the thermally reversible swelling/deswelling behavior of the hydrogel coating. Our strategy utilizes surfactant-free emulsion polymerization (SFEP) to grow the hydrogel coating (Scheme 1) [Saunders and Vincent, 1999; Saunders et al., 1997; Kawaguchi et al., 1992; Corpart and Candau, 1993; Neyret and Vincent, 1997; Ole Kiminta et al., 1995]. This approach enables us to produce stable, chemically-resistant polymer shells on gold nanoparticle cores [Kreibig and Vollmer, 1995]. The long-range goal of this research is to prepare and characterize discrete nanoscale drug-delivery vehicles comprised of biocompatible hydrogel-coated gold particles in which volume transitions lead to drug-release. Ultimately, we wish to use composite gold nanoparticle cores in which tissue-transparent near-IR light can be used to excite the plasmon resonance of the cores [Sershen et al., 2000; Pham et al., 2002]. The heat generated by near-IR excitation will collapse a drug-impregnated hydrogel overlayer, giving rise to drug release [Sershen et al., 2000; Zhu et al., 2004; Gorelikov et al., 2004; Kim and Lee, 2004a,b].

EXPERIMENTAL DETAILS

Materials

The N-isopropylacrylamide (NIPAM) monomer (Acros, 99%) was recrystallized in hexane and dried under vacuum before use. Co-monomer acrylic acid (AAc, Acros, 99.5%), crosslinker N,N-methylenebisacrylamide (BIS, Acros, 96%), potassium hydroxide (KOH, 85%), nitric acid, uranyl acetate dihydrate, ammonium persulfate (APS, EM, 98%), and oleic acid (OA, J.T. Baker) were used as received from the indicated suppliers. Water used in all reactions was purified to a resistance of 18 MΩ (Academic Milli-Q Water System; Millipore Corporation, Bedford, MA) and filtered through a 0.22-μm membrane filter to

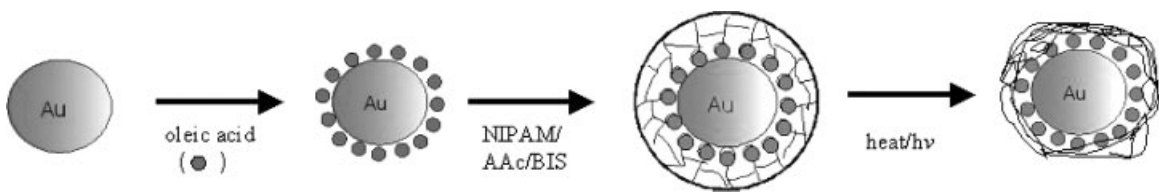

Scheme 1. Hydrogel growth process using surfactant-free emulsion polymerization.

remove any impurities. Trisodium citrate (EM, 99%) and hydrogen tetrachloroaurate (Strem, Au 99.9%) were used without purification to prepare the gold nanoparticle cores.

Synthesis of Gold and Hydrogel-Coated Gold Nanoparticles

Large gold nanoparticles (55–65 nm diameter) were prepared using the citrate reduction method, which has been described elsewhere [Frens, 1973; Turkevich et al., 1951; Goodman et al., 1981]. The glassware was cleaned with strong acid and then with strong base (saturated KOH in isopropyl alcohol) before use. The resultant nanoparticle cores were briefly characterized by dynamic light scattering (DLS) and field emission scanning electron microscopy (FE-SEM) before further use.

The preparation of hydrogel-coated gold nanoparticles was accomplished by SFEP in aqueous solution. Gold colloidal solutions were diluted with purified Milli-Q water to give a UV-vis maximum of ~0.25 a.u. at 530 nm and transferred to a three-necked round-bottomed flask equipped with a reflux condenser and an inlet for argon. The solution was vigorously stirred, and argon was bubbled through the solution for 1 h to completely remove any oxygen, which can intercept radicals and disrupt the polymerization process. An aliquot (1.6 mL of a 0.001 M solution; 0.002 mmol) of oleic acid was added to the gold solution under argon. The mixture was stirred for another 1 h and ultrasonicated for 10 min. An approximately 94:6 wt% ratio of NIPAM (26.1 mL of a 0.01 M solution; 0.26 mmol) to AAc (1.6 mL of a 0.01 M solution; 0.02 mmol) was then added with 1.3 mL of a 0.01 M solution (0.01 mmol) of crosslinker BIS and stirred for 15 min to give homogeneity. The solution was then heated to 70°C and then the initiator APS 0.8 mL of a 0.01 M solution (0.008 mmol) was added to start the polymerization. The reaction time was varied between 6 and 8 h depending on the starting materials. The final solution was purified by filtration using a 0.45-μm membrane filter to remove any micron-sized impurities and/or any aggregated particles at the end of the reaction. The solution was centrifuged at 20°C for 2 h at 3,500 rpm with an RC-3B refrigerated centrifuge (Sorvall Instruments), and the supernatant was carefully separated to remove any unreacted materials, soluble side products, and oligomers. The purified nanoparticles were then diluted with Milli-Q water and stored in a refrigerator for later analysis. The thickness of the hydrogel coating was varied between 20 and 90 nm depending on the reaction time and the amounts of the initiator and the monomers.

Characterization of Gold and Hydrogel-Coated Gold Nanoparticles

To characterize fully the morphology and elemental composition of the gold nanoparticle cores and hydrogel-coated gold nanoparticles, we used field emission scanning electron microscopy (FE-SEM), transmission electron microscopy (TEM), and energy dispersive X-ray (EDX) analysis. The optical properties were measured by ultraviolet-visible (UV-vis) spectroscopy, and the hydrodynamic diameters were measured by dynamic light scattering (DLS).

We used a Cary 50 Scan UV-vis optical spectrometer (Varian) equipped with Cary Win UV software to observe the optical properties of the bare gold nanoparticles and the different thickness of the hydrogel-coated gold nanoparticles. UV-vis spectra of the gold nanoparticles were collected by diluting the particles with pure water, transferring them to an optical quartz cell, and scanning over a range of wavelengths. The hydrogel-coated gold nanoparticles were analyzed without dilution. UV-vis spectra of the distinct batches of nanoparticles were collected both before and after coating with the hydrogel polymer for experimental consistency.

Morphological and elemental analysis by FE-SEM was performed using a JSM 6330F (JEOL) instrument operating at 15 kV and equipped with a setup for elemental analysis by EDX (Link ISIS software series 300, Oxford Instruments). For the FE-SEM images and the EDX spectra, the gold nanoparticles and hydrogel-coated gold nanoparticles were placed on Formvar-coated copper grids. All samples were dried at room temperature overnight before analysis. To give homogeneous electron distributions, the samples were coated with carbon using a vacuum sputterer. The gold and hydrogel-coated gold nanoparticles were characterized by FE-SEM to show the overall morphological features and by EDX to support the presence of the gold nanoparticle cores.

Analysis by TEM was accomplished using a JEM-2000 FX electron microscope (JEOL) operating at an accelerating voltage of 200 kV. The samples were selectively stained with uranyl acetate on the AAc groups. All TEM samples were deposited on 300 mesh Holey carbon-coated copper grids and dried before analysis.

For measuring the hydrodynamic diameters of bare gold nanoparticles and hydrogel-coated gold nanoparticles as a function of temperature and pH, a DLS instrument (ALV-5000 Multiple Tau Digital Correlation) operating at a light source wavelength of 514.5 nm and a fixed scattering angle of 90° was used. These measurements were carefully conducted at

dilute concentrations with precise control over the temperature to reduce artifacts arising from convection currents in the samples. Data were recorded from 20–60°C for all samples.

DISCUSSION

Hydrogel-coated gold nanoparticles were reproducibly prepared by SFEP at 70°C in aqueous solution. We found that this method was convenient for the hydrogel-coating process because all starting reagents and products are soluble under the reaction conditions and there is no need for purification steps during the polymerization process. One disadvantage of this strategy is that phase separation can easily occur during the polymerization if the reaction conditions are varied widely. Using this method, we were able to prepare stable gold nanoparticles (~60 nm diameter) coated with a hydrogel overlayer (20–90 nm thick). These hybrid nanoparticles were stable without aggregation for more than two to three months at room temperature. Moreover, in our hands, thin hydrogel coatings were more reproducibly prepared than thick hydrogel coatings. Gold nanoparticles with hydrogel coatings less than 50 nm thick were reliably prepared without side products, while those with the thicker coatings (more than 50 nm) were sometimes prepared in pure form (~50% of the time) and sometimes prepared with the concomitant formation of pure hydrogel particles with no gold cores.

The UV-vis absorption spectra of bare gold nanoparticles and hydrogel-coated gold nanoparticles are shown in Figure 1. It is known that gold nanoparticles exhibit an absorption maximum at 530–540 nm arising from the gold plasmon resonance [Link and El-Sayed, 1999]. The observation of this band in Figure 1 supports the presence of gold nanoparticles in our samples. Moreover, the unsymmetrical band centered at 535 nm is consistent with the formation of spherical gold nanoparticles described elsewhere [Rivas et al., 2001]. The position and shape of the plasmon resonance are affected by the particle size, shape, and particle surroundings [Underwood and Mulvaney, 1994; Mie, 1908]. The UV-vis spectra of solutions of hydrogel-coated gold nanoparticles are similar to those of NIPAM homopolymer-coated gold nanoparticles or silica-coated gold nanoparticles [Liz-Marzan et al., 1996]. When the thickness of the hydrogel coating on the gold nanoparticle increases, the gold plasmon resonance remains unshifted in position but decreases in intensity (see Fig. 1) because the refractive index of the hydrogel copolymer is different from the surrounding medium (water) and that of the core material (gold nanoparticles). The observed correlation suggests enhanced UV scattering

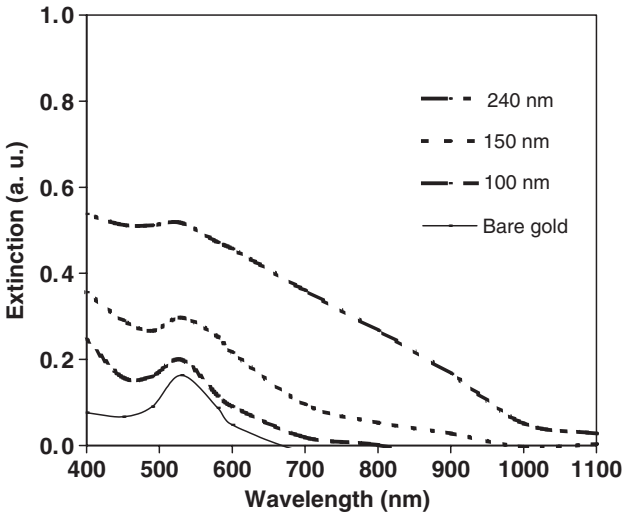

Fig. 1. U.V-visible spectra of bare gold nanoparticles and hydrogel-coated gold nanoparticles.

with increasing hydrogel polymer thickness; scattering seems to dominate at shorter wavelengths for the thicker coatings, causing an apparent weakening of the gold plasmon band. This behavior is largely consistent with core-shell nanoparticle studies by Aden and Kerker [1951], which represents a modification of Mie scattering theory [Mie, 1908].

Figure 2 shows FE-SEM micrographs of the gold nanoparticles and hydrogel-coated gold nanoparticles prepared in this study. The images in Figure 2 show that all of the gold nanoparticles are highly spherical, but the hydrogel-coated nanoparticles are more irregularly shaped, particularly for those having thicker coatings. Furthermore, a small percentage of the hydrogel-coated nanoparticles contain two or three gold cores. We have also found that the use of a surfactant (sodium dodecyl sulfate) in the polymerization process affords smoother surfaces but thinner coatings. The surfaces of the gold particles seem to be completely coated because we observed no bare gold nanoparticle cores among the hydrogel particles.

We obtained EDX spectra from the same samples used above to collect the FE-SEM images. Figure 3 provides a representative spectrum; all samples show similar EDX data. These analyses confirmed the presence of characteristic gold peaks (Mα, Lα) at 2.12 and 9.71 keV, respectively, and additional copper peaks arising from the supporting copper grid. The intensities of the gold peaks for the hydrogel-coated nanoparticles were weaker than those for bare gold nanoparticles measured at the same energy level. In addition, pure hydrogel particles without gold cores showed only the presence of copper. Collectively, the

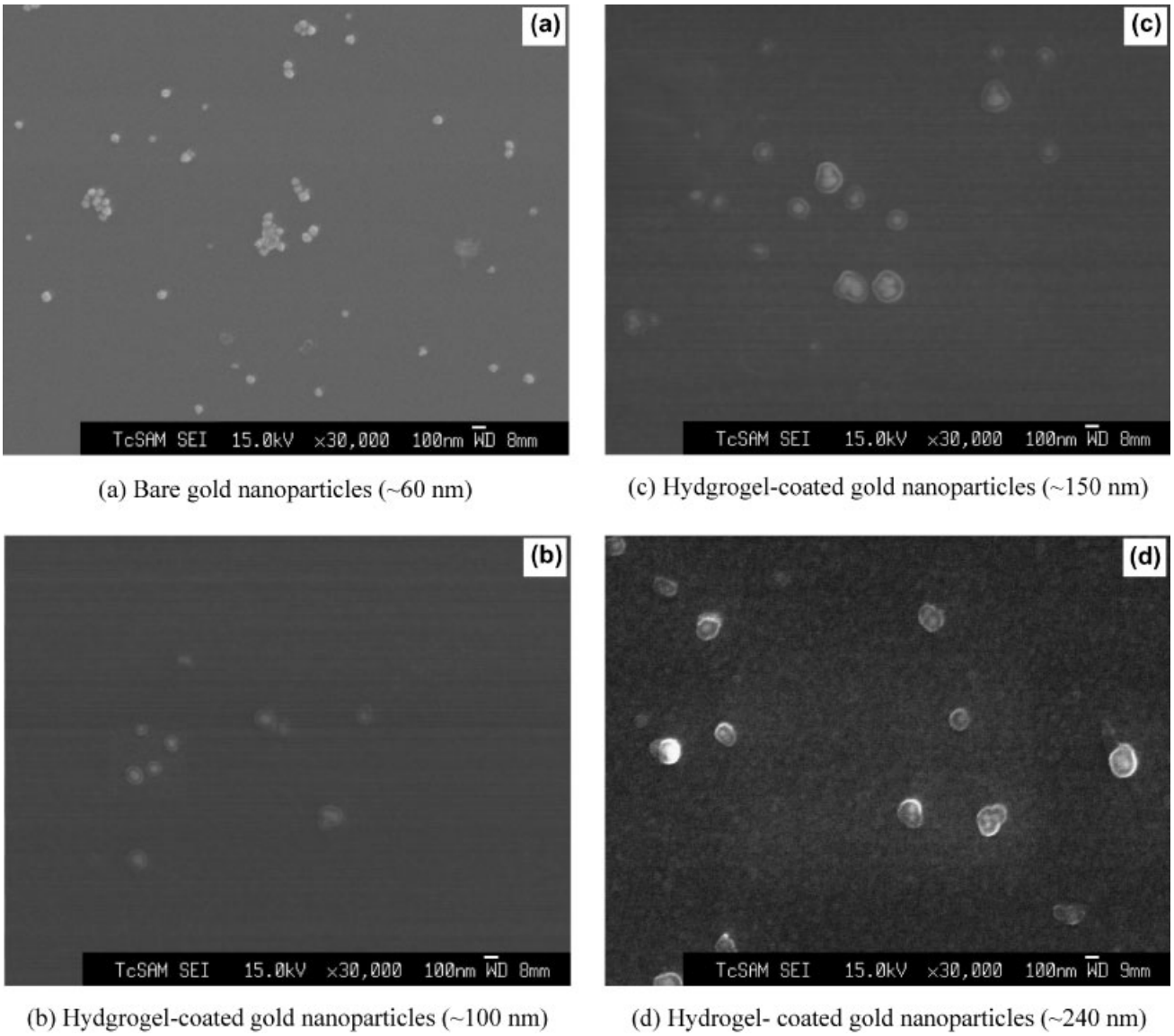

Fig. 2. FE-SEM micrographs of (**a**) bare gold and (**b–d**) hydrogel-coated gold nanoparticles with varying hydrogel thickness.

EDX analyses support the formation of hydrogel-coated gold nanoparticles.

TEM images of hydrogel-coated gold nanoparticles are shown in Figure 4. To detect the hydrogel coatings on the gold nanoparticle cores, the AAc groups in the hydrogel polymers were selectively coated through negative staining with 1% uranyl acetate. This treatment was necessary because the polymer layer has insufficient electron density for direct analysis by TEM. The hydrogel coating appears as a cloudy white layer between the gold core and the background. Thin coatings follow the shape of the gold nanoparticles; thicker ones tend to possess irregular shapes due to the collapse of the hydrogel under high vacuum and electron beam bombardment. These phenomena are also responsible for the smaller measured sizes of the hydrogel-coated gold nanoparticles when compared to measurements by DLS (vide infra).

We used DLS to obtain the hydrodynamic diameters of the bare gold nanoparticles and the ~150-nm hydrogel-coated gold nanoparticles as a function of pH and temperature. We found an increase in the diameter of the hydrogel-coated gold nanoparticles with increasing pH (see Fig. 5). Bare gold nanoparticles were unaffected by pH, but the hydrogel-coated gold nanoparticles showed a systematic ~40 nm variability in the diameter. It is known that the pH range for the swelling-deswelling transition of

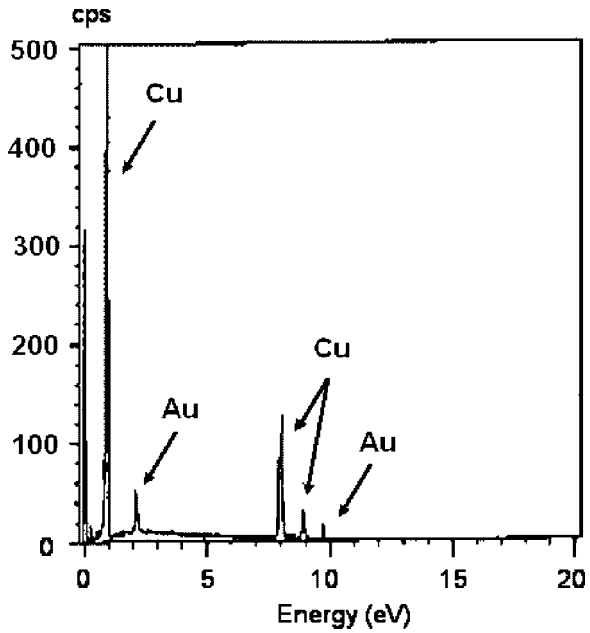

Fig. 3. EDX spectrum of hydrogel-coated gold nanoparticles.

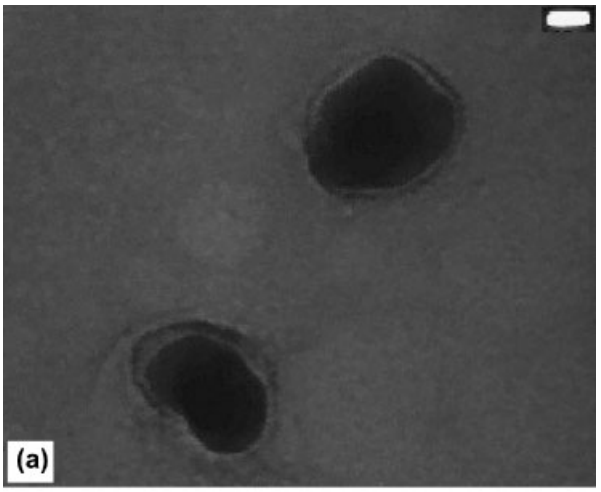

(a) Hydgrogel-coated gold nanoparticles (~100 nm)

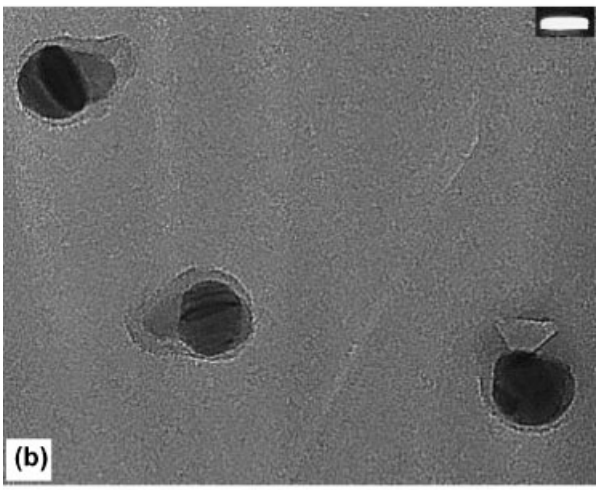

(b) Hydgrogel-coated gold nanoparticles (~150 nm)

Fig. 4. TEM micrographs of (**a**) ~100 nm of hydrogel-coated gold nanoparticles and (**b**) ~150 nm of hydrogel-coated gold nanoparticles. Scale bars = (a) 20 nm, (b) 50 nm.

the hydrogel-coated gold nanoparticles occurs between pH 3 and 6, which is consistent with the pKa value of acrylic acid (4.25) [Morris et al., 1997]. The particles shrink dramatically due to neutralization of the carboxylate groups under acidic conditions. Under basic conditions, the hydrogel-coated gold nanoparticles are swollen because of internal electrostatic repulsion among anionic carboxylate groups in the hydrogel polymer matrix. The continuous rather than sudden increase in the observed swelling behavior can be attributed to a random distribution of ionizable groups in the polymer backbone [Morris et al., 1997].

Figure 6 illustrates the hydrodynamic diameter changes of the bare gold and hydrogel-coated gold nanoparticles under neutral pH as a function of temperature. The diameters of the bare gold nanoparticles remain constant, while the diameters of the hydrogel-coated gold nanoparticles decrease with increasing temperature. Deswelling of the hydrogel polymer layer at elevated temperatures is caused by the loss of hydrogen bonding between water and the hydrophilic sites (−C = O, −NH−) along the hydrogel polymer backbone [Shibayama et al., 1996]. The thermally-activated loss of hydrogen bonding in the hydrogel polymer matrix eliminates internal electrostatic repulsion, leading to a collapse of the swelled structure [Shibayama et al., 1996]. The electrostatic circumstance can be adjusted by adding ionizable groups, such as acrylic acid moieties, along the polymer backbone. The presence of water molecules and hydrophilic sites in the solution gives rise to hydrogen-bonding interactions within hydrogel polymer matrix at low temperatures, permitting electrostatic repulsion to influence the water-swelling and/or deswelling behavior [Kato, 1997].

It is known that the LCST of NIPAM hydrogel homopolymers is ~32°C [Pelton et al., 1989; Tan et al., 1992], but our hydrogel-coated gold nanoparticles possess 6% acrylic acid moieties, which should broadly increase the LCST to ~34–40°C according to previous studies [Morris et al., 1997]. For our samples, however, increasing the temperature above 30°C led to a gradual decrease in the hydrodynamic diameter of the particles, which became constant above 45°C (see Fig. 6). We also observed that variations in temperature induce

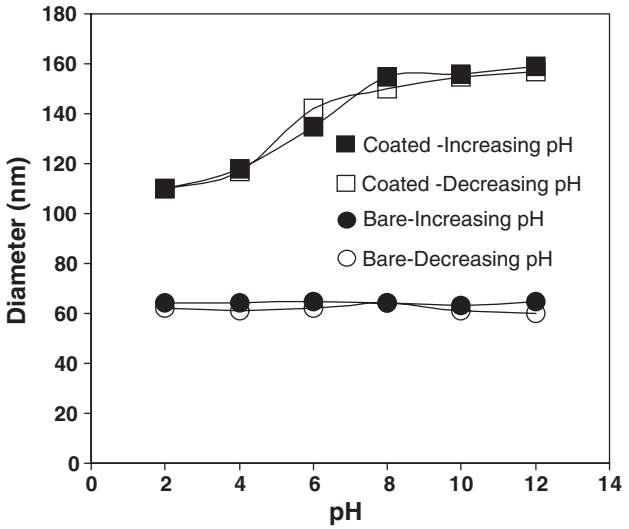

Fig. 5. The hydrodynamic diameter changes of bare gold nanoparticles and hydrogel-coated gold nanoparticles as a function of pH. Filled symbols correspond to increasing pH; open symbols correspond to decreasing pH.

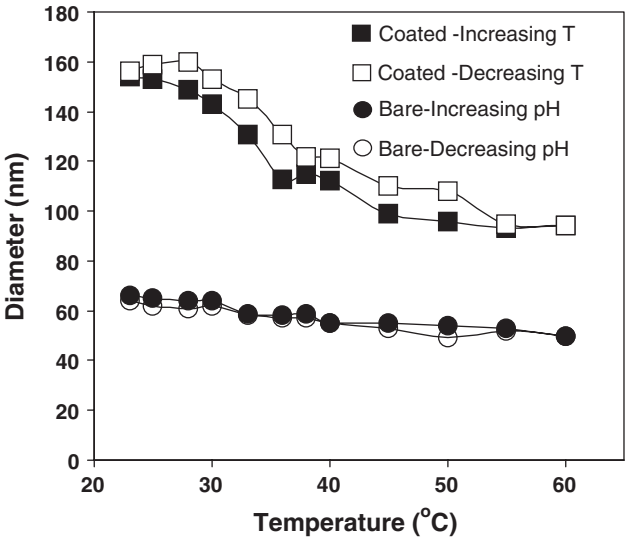

Fig. 6. The hydrodynamic diameter changes of bare gold nanoparticles and hydrogel-coated gold nanoparticles as a function of temperature. Filled symbols correspond to increasing temperature; open symbols correspond to decreasing temperature.

a greater change in the hydrodynamic diameter of the hydrogel-coated gold nanoparticles than do variations in pH. This observation suggests that the particle swelling and deswelling behavior is dominated more by the NIPAM component than the pH-dependent size changes effected by the AAc component, given that the hydrogel co-polymer consists of 94% NIPAM.

CONCLUSIONS

This work describes the encapsulation of gold nanoparticles within a thermo-and pH-responsive biocompatible hydrogel polymer shell. The gold cores were ~60 nm in diameter, and the thickness of the hydrogel overlayer could be varied from 20 to 90 nm depending on the reaction time and the relative amounts of the initiator and monomers. Analysis of the morphology, elemental composition, and optical properties of the composite nanoparticles support the formation of discrete hydrogel-coated gold nanoparticles. Measurements by DLS revealed volume changes in the polymer layer as a function of pH and temperature; in particular, the hydrodynamic diameters of the hydrogel-coated gold nanoparticles were observed to decrease with decreasing pH and increasing temperature. Our studies demonstrate that these composite nanoparticles can be readily prepared through the SFEP method and that their responses to changes in external stimuli (temperature and pH) are consistent with their targeted use as photothermally activated drug-delivery vehicles. For this application, the photosensitive core materials must possess strong optical absorptions in the "water window" (800–1,200 nm) [Sershen et al., 2000; Simpson et al., 1998]. Consequently, rather than simple metal nanoparticle cores, we will employ core-shell metal nanoparticles and/or metal nanorods, which can be tailored to possess optical absorptions at suitable wavelengths [Pham et al., 2002; Gorelikov et al., 2004].

ACKNOWLEDGMENTS

We thank Dr. J.K. Meen for assistance with the FE-SEM measurements, Dr. I. Rusakova for assistance with the TEM measurements, and Dr. J.C. Reina for assistance with the DLS measurements.

REFERENCES

Aden AL, Kerker M. 1951. Scattering of electromagnetic waves from two concentric spheres. J Appl Phys 22:1242–1246.

Alivisatos AP. 1996. Semiconductor clusters, nanocrystals, and quantum dots. Science 271:933–937.

Bergbreiter DE, Case BL, Liu YS, Caraway JW. 1998. Poly(N-isopropylacrylamide) soluble polymer supports in catalysis and synthesis. Macromolecules 31:6053–6062.

Bohren CF, Hoffman DR. 1998. Absorption and scattering of light by small particles. New York: Wiley, p 82–129.

Chen S, Sommers JM. 2001. Alkanethiolate-protected copper nanoparticles: spectroscopy, electrochemistry, and solid-state morphological evolution. J Phys Chem B 105:8816–8820.

Clark HA, Campagnok PJ, Wuskell JP, Lewis A, Loew LM. 2000. Second harmonic generation properties of fluorescent polymer-encapsulated gold nanoparticles. J Am Chem Soc 122: 10234–10235.

Corpart JM, Candau F. 1993. Formulation and polymerization of microemulsions containing a mixture of cationic and anionic monomers. Colloid Polym Sci 271:1055–1067.

Frens G. 1973. Controlled nucleation for the regulation of the particle size in monodisperse gold suspensions. Nature (London) Phy Sci 241:20–22.

Goodman SL, Hodges GH, Trejdosiewicz LK, Linvinton DC. 1981. Colloidal gold markers and probes for routine application in microscopy. J Microsc 123:201–213.

Gorelikov I, Field LM, Kumacheva E. 2004. Hybrid microgels photoresponsive in the near-infrared spectral range. J Am Chem Soc 126:15938–15939.

Jeong B, Bae YH, Lee DS, Kim SW. 1997. Biodegradable block copolymers as injectable drug-delivery systems. Nature 388: 860–862.

Jones CD, Lyon LA. 2000. Synthesis and characterization of multiresponsive core-shell microgels. Macromolecules 33: 8301–8306.

Jones CD, Lyon LA. 2003a. Photothermal patterning of microgel/gold nanoparticle composite colloidal crystals. J Am Chem Soc 125:460–465.

Jones CD, Lyon LA. 2003b. Shell-restricted swelling and core compression in poly(N-isopropylacrylamide) core-shell microgels. Macromolecules 36:1988–1993.

Kato E. 1997. Volume-phase transition of N-isopropylacrylamide gels induced by hydrostatic pressure. J Chem Phys 106: 3792–3797.

Kawaguchi H, Fujimoto K, Mizuhara, Y. 1992. Hydrogel microspheres. III. Temperature-dependent adsorption of proteins on poly(N-isopropylacrylamide) hydrogel microspheres. Colloid Polym Sci 270:53–57.

Kim JH, Lee TR. 2004a. Hydrogel-coated gold nanoparticles. PMSE Preprints 90:637–638.

Kim JH, Lee TR. 2004b. Thermo- and pH-responsive hydrogel-coated gold nanoparticles. Chem Mater 16:3647–3651.

Kreibig U, Vollmer M. 1995. Optical properties of metal clusters; Springer Series in Material Science 25. Berlin: Springer. p 1–12.

Link S, El-Sayed MA. 1999. Size and temperature dependence of the plasmon absorption of colloidal gold nanoparticles. J Phys Chem B 103:4212–4217.

Liz-Marzan LM, Giersig M, Mulvaney P. 1996. Synthesis of nanosized gold-silica core-shell particles. Langmuir 12: 4329–4335.

Maier SA, Brongersma ML, Kik PG, Meltzer S, Requicha AAG, Koel BE, Atwater HA. 2001. Plasmonics-A route to nanoscale optical devices. Adv Mater 13:1502–1505.

Merchant B. 1998. Gold, the noble metal and the paradoxes of its toxicology. Biologicals 26:49–59.

Mie G. 1908. Contributions to the optics of turbid media, especially colloidal metal solutions. Ann Phys 25:377–445.

Morris GE, Vincent B, Snowden MJ. 1997. Adsorption of lead ions onto N-isopropylacrylamide and acrylic acid copolymer microgels. J Colloid Interface Sci 190:198–205.

Nayak S, Lyon LA. 2004. Photoinduced phase transitions in poly(N-isopropylacrylamide) microgels. Chem Mater 16:2623–2627.

Neyret S, Vincent B. 1997. The properties of polyampholyte microgel particles prepared by microemulsion polymerization. Polymer 38:6129–6134.

Ole Kiminta DM, Luckham PF, Lenon S. 1995. The rheology of deformable and thermoresponsive microgel particles. Polymer 36: 4827–4831.

Pelton R. 2000. Temperature-sensitive aqueous microgels. Adv Colloid Interface Sci 85:1–33.

Pelton RH, Pelton HM, Morphesis A, Rowell RL. 1989. Particle sizes and electrophoretic mobilities of poly(N-isopropylacrylamide) latex. Langmuir 5:816–818.

Pham T, Jackson JB, Halas NJ, Lee TR. 2002. Preparation and characterization of gold nanoshells coated with self-assembled monolayers. Langmuir 18:4915–4920.

Quanroni L, Chumanov G. 1999. Preparation of polymer-coated functionalized silver nanoparticles. J Am Chem Soc 121: 10642–10643.

Rivas L, Sanchez-Cortes L, Garcia-Ramos JV, Morcillo G. 2001. Growth of silver colloidal particles obtained by citrate reduction to increase the Raman enhancement factor. Langmuir 17: 574–577.

Saunders BR, Crowther HM, Vincent B. 1997. Poly[(methyl methacrylate)-co-(methacrylic acid)] microgel particles: swelling control using pH, cononsolvency, and osmotic deswelling. Macromolecules 30:482–487.

Saunders BR, Vincent B. 1996. Thermal and osmotic deswelling of poly(NIPAM) microgel particles. J Chem Soc Faraday Trans 92: 3385–3389.

Saunders BR, Vincent B. 1999. Microgel particles as model colloids: theory, properties and applications. Adv Colloid Interface Sci 80: 1–25.

Schild HG, Tirrell DA. 1990. Microcalorimetric detection of lower critical solution temperatures in aqueous polymer solutions. J Phys Chem 94:4352–4356.

Sershen SR, Westcott SL, Halas NJ, West JL. 2000. Temperature-sensitive polymer–nanoshell composites for photothermally modulated drug delivery. J Biomed Mat Res 51: 293–298.

Shibayama M, Mizutani S, Nomura S. 1996. Thermal properties of copolymer gels containing N-isopropylacrylamide. Macromolecules 29:2019–2024.

Simpson CR, Kohl M, Essenpreis M, Cope M. 1998. Near-infrared optical properties of ex vivo human skin and subcutaneous tissues measured using the Monte Carlo inversion technique. Phys Med Biol 43:2465–2478.

Snowden MJ, Tomas D, Vincent B. 1993. Use of colloidal microgels for the absorption of heavy metal and other ions from aqueous solution. Analyst 118:1367–1369.

Snowden MJ, Chowdhry BZ, Vincent B, Morris GE. 1996. Colloidal copolymer microgels of N-isopropylacrylamide and acrylic acid: pH, ionic strength and temperature effects. J Chem Soc Faraday Trans 92:5013–5016.

Sun Y, Xia Y. 2002. Increased sensitivity of surface plasmon resonance of gold nanoshells compared to that of gold solid colloids in response to environmental changes. Anal Chem 74: 5297–5305.

Tan KC, Wu XY, Pelton RH. 1992. Viscometry: a useful tool for studying conformational changes of poly(N-isopropylacrylamide) in solutions. Polymer 33:436–438.

Teranishi T, Miyake M. 1998. Size control of palladium nanoparticles and their crystal structures. Chem Mater 10: 594–600.

Turkevich J, Stevenson PC, Hillier J. 1951. The nucleation and growth processes in the synthesis of colloidal gold. Discussions Fara Soc 58:55–75.

Underwood S, Mulvaney P. 1994. Effect of the solution refractive index on the color of gold colloids. Langmuir 10:3427–3430.

Yoshida R, Sakai K, Okano T, Sakuri Y. 1994. Modulating the phase transition temperature and thermosensitivity in N-isopropylacrylamide copolymer gels. J Biomater Sci Polym Ed 6: 585–598.

Zhou S, Chu B. 1998. Synthesis and volume phase transition of poly(methacrylic acid-co-N-isopropylacrylamide) microgel particles in water. J Phys Chem B 102:1364–1371.

Zhu MQ, Wang LQ, Exarhos GJ, Li ADQ. 2004. Thermosensitive gold nanoparticles. J Am Chem Soc 126:2656–2657.